



Article

# Genomic Variations in Susceptibility to Intracranial Aneurysm in the Korean Population

Eun Pyo Hong <sup>1,2</sup> , Bong Jun Kim <sup>2</sup>, Steve S. Cho <sup>3</sup>, Jin Seo Yang <sup>4</sup>, Hyuk Jai Choi <sup>4</sup>, Suk Hyung Kang <sup>4</sup> and Jin Pyeong Jeon <sup>2,4,5,\*</sup>

<sup>1</sup> Molecular Neurogenetics Unit, Center for Genomic Medicine, Massachusetts General Hospital, Boston, MA 02114, USA; ephong0305@gmail.com

<sup>2</sup> Institute of New Frontier Stroke Research, Hallym University College of Medicine, Chuncheon 24252, Korea; luckykbj@naver.com

<sup>3</sup> Perelman School of Medicine at the University of Pennsylvania, Philadelphia, PA 19104, USA; swcho92@gmail.com

<sup>4</sup> Department of Neurosurgery, Hallym University College of Medicine, Chuncheon 24252, Korea; yiyaseo@naver.com (J.S.Y.); painsurgery@gmail.com (H.J.C.); nscharisma@daum.net (S.H.K.)

<sup>5</sup> Genetic and Research, Chuncheon 25252, Korea

\* Correspondence: jjs6553@daum.net; Tel.: +82-33-240-5171; Fax: +82-33-240-9970

Received: 18 January 2019; Accepted: 21 February 2019; Published: 25 February 2019



**Abstract:** Genome-wide association studies found genetic variations with modulatory effects for intracranial aneurysm (IA) formations in European and Japanese populations. We aimed to identify the susceptibility of single nucleotide polymorphisms (SNPs) to IA in a Korean population consisting of 250 patients, and 294 controls using the Asian-specific Axiom Precision Medicine Research Array. Twenty-nine SNPs reached a genome-wide significance threshold ( $5 \times 10^{-8}$ ). The rs371331393 SNP, with a stop-gain function of *ARHGAP32* (11q24.3), showed the most significant association with the risk of IA (OR = 43.57, 95% CI: 21.84–86.95;  $p = 9.3 \times 10^{-27}$ ). Eight out of 29 SNPs—*GBA* (rs75822236), *TCF24* (rs112859779), *OLFML2A* (rs79134766), *ARHGAP32* (rs371331393), *CD163L1* (rs138525217), *CUL4A* (rs74115822), *LOC102724084* (rs75861150), and *LRRC3* (rs116969723)—demonstrated sufficient statistical power greater than or equal to 0.8. Two previously reported SNPs, rs700651 (*BOLL*, 2q33.1) and rs6841581 (*EDNRA*, 4q31.22), were validated in our GWAS (Genome-wide association study). In a subsequent analysis, three SNPs showed a significant difference in expressions: the rs6741819 (*RNF144A*, 2p25.1) was down-regulated in the adrenal gland tissue ( $p = 1.5 \times 10^{-6}$ ), the rs1052270 (*TMOD1*, 9q22.33) was up-regulated in the testis tissue ( $p = 8.6 \times 10^{-10}$ ), and rs6841581 (*EDNRA*, 4q31.22) was up-regulated in both the esophagus ( $p = 5.2 \times 10^{-12}$ ) and skin tissues ( $1.2 \times 10^{-6}$ ). Our GWAS showed novel candidate genes with Korean-specific variations in IA formations. Large population based studies are thus warranted.

**Keywords:** subarachnoid hemorrhage; delayed cerebral ischemia; genetics

## 1. Introduction

Intracranial aneurysms (IAs), formed through the ballooning of intracranial arteries, are reported with an overall prevalence of 3.2% [1]. While annual rupture rates of up to 2% have been reported, subarachnoid hemorrhage (SAH) due to an aneurysm rupture is a life-threatening illness with a one-month mortality rate of up to 50% [2]. IAs represent a complex dysfunction with clinical implications and genetic components. Highly associated clinical risk factors for IA are sex (female), hypertension, and smoking [3]. The associations between IA and some heritable conditions, such as autosomal dominant polycystic kidney disease, Marfan syndrome, and Ehlers-Danlos syndrome,

as well as family histories of IA suggest some possible genetic contributions to IA formation [4]. In particular, candidate loci such as 1p34.3-p36.13, 7q11, 19q13.3, and Xp22 have been reported in familial IA [4–8].

As of late 2008, previous genome-wide association studies (GWASs) have identified single nucleotide polymorphisms (SNPs) located within or near several candidate genes, including *EDNRA*, *SOX17*, *CDKN2A*, and *RBBP8*, which reached a genome-wide significance or suggestive threshold for the susceptibility to IA formation [9–12]. A meta-analysis of 61 studies in multi-ethnic populations further [13] demonstrated regions 4q31.23, 9p21.3, and 8q11 to be significantly associated with IA. Despite attempts to discover casual or candidate genes for IA formation or SAH development via GWAS-driven approaches, most of these studies have been conducted in both European and Asian-ancestry populations using the large-scale SNP array manufactured on the basis of Caucasian populations. Since the existence of ethnic difference should be considered in the fundamental identification of genomic susceptibility to complex diseases in multi-ethnic populations [14], even with in the same ethnicity, such as Japanese and Korean populations [15], the impact of susceptible loci on IA in the Korean populations remains to be clarified.

Recently, The Axiom Asia Precision Medicine Research Array (PMRA), a comprehensive imputation-aware genotyping array on the basis of South- and East Asian populations, which contains more than 750,000 markers including disease-associated rare or common variations cataloged in public databases such as ClinVar and GWAS Catalog (Thermo Fisher Scientific, Waltham, MA, USA), was launched in South Korea and led to a new paradigm in genomic research. In this study, we aimed to identify IA-predicting genetic variations in Korean adults based on hospitalization records for SAH and IA. To the best of our knowledge, this study is the first GWAS report applying the Asian-specific PMRA chip to provide a better understanding of IA formation.

## 2. Materials and Methods

### 2.1. Study Population

The study cohort was derived from the Chuncheon Sacred Heart Hospital stroke database (2015–2018). This database is a prospective and observational project in the regional medical center of the district of Chuncheon city, the capital city of the Gangwon Province in Korea [16]. Patients with a clinical diagnosis and neuroimaging consistent with hemorrhagic or ischemic strokes were recruited for the database. In this GWAS study, patients over 18 years of age with saccular and sporadic IA were analyzed. Non-saccular aneurysms, such as fusiform, dissection, traumatic, and infectious aneurysms, as well as familial aneurysms were excluded. Control subjects met the following criteria: 1) they underwent computed tomography or magnetic resonance angiography for headache evaluation or medical check-up; 2) had no concomitant neurological diseases, such as arteriovenous malformation, intracranial hemorrhage, or infarct; 3) had no familial history of IA or SAH in first-degree relatives; 4) had neither Parkinson's disease (PD) or Alzheimer's disease; and 5) were over 18 years of age [17,18]. Finally, this prospective study included radiologically confirmed IA with saccular shape ( $n = 250$ ) and 296 controls enrolled from March 2015 to May 2018 at a single institution. Medical information was reviewed regarding sex, age, present symptoms (UIA or SAH), hypertension (HTN), diabetes mellitus (DM), hyperlipidemia, smoking, familial history of aneurysm, and the presence of SAH. Angiographic variables were reviewed concerning the aneurysm location (anterior vs. posterior) and size. This study was approved by the Institutional Review Board at the participating hospital (No. 2016-3, 2017-9).

### 2.2. Genotyping and Sample Quality Control

Genomic DNA from peripheral blood was extracted using the HiGene™ Genomic DNA Prep Kit (BIOFACT, Daejeon, Korea). The samples were genotyped using the Axiom™ Asia Precision Medicine Research Array (PMRA) Kit (Thermo Fisher Scientific, Waltham, MA, USA), which contains over 750,000 SNPs including 50,000 novel markers covering East and South Asian populations based

on the human genome version 19 (build 37). A total of 508,192 out of 798,148 variants, including small insertions/deletions (indels), passed the quality control test with a genotype call rate of  $\geq 95\%$ , minor allele frequency (MAF)  $\geq 0.01$ , and Hardy-Weinberg equilibrium  $p$ -value  $\geq 1 \times 10^{-6}$ , and these were tested in our GWAS.

### 2.3. Statistical Analysis

A descriptive analysis is shown using the numbers of subjects (percentage) for discrete and categorical variables, and means are shown with standard errors. We conducted a multivariate logistic analysis with seven confounding factors (sex, age, HTN, DM, hyperlipidemia, cigarette smoking, and four principal components) in 250 cases with IA and 294 controls after removing two missing values. These analyses were performed using STATA v11.2 (Stata Corp., Lakeway, TX, USA). Our genome-wide association analysis was conducted to identify candidate genetic variations for IA susceptibility under an additive inheritance effect model, after adjusting for ten potential covariates mentioned above using the PLINK 1.9 program (<https://www.cog-genomics.org/plink/1.9/>) [19]. We estimated the statistical power to evaluate a potential genetic reliability in GWAS using our candidate genetic variants demonstrating genome-wide associations with the Genetic Power Calculator (<http://pngu.mgh.harvard.edu/~jpurcell/gpc/>), based on the following assumptions: an IA prevalence of 5%, an odds-ratio (OR) in an additive effect model, a D-prime of 0.8, a 1:1.18 case-control ratio, and a type 1 error rate at a genome-wide significance level of  $5 \times 10^{-8}$ . We further evaluated the genetic associations between 151 SAH and 99 UIA patients in a subsequent analysis. In addition, we analyzed single tissue expression quantitative trait loci (eQTL) to evaluate genetic effects on the expression levels of individual variants demonstrating genome-wide associations in our GWAS through the Genotype-Tissue Expression (GTEx v7) portal (<https://gtexportal.org/home/>) [20]. Manhattan and regional association plots were drawn by the “*qqman*” command in R package v3.4.0 (<https://cran.r-project.org/web/packages/qqman>) and LocusZoom v1.3 (<http://locuszoom.org/>), respectively [21].

### 2.4. Gene Functional Enrichment, Pathway, and Network Analyses

We analyzed the enrichment of gene ontology (GO) terms and Kyoto Encyclopedia of Genes and Genomes (KEGG) pathways, in order to functionally classify candidate genes for IA susceptibility with  $p$ -values less than 0.05 that were identified in our GWA analysis. For this we used the web-based program Database for Annotation, Visualization, and Integrated Discovery (DAVID) v6.8 (<http://david.ncifcrf.gov/>) [22]. Biological functions with a false discovery rate (FDR) of less than 0.01 were considered to be strongly enriched in the annotation categories. We displayed the functional association network of the identified proteins in the pathogenesis of IA formation using STRING v10 (<http://string-db.org/>) [23].

## 3. Results

### 3.1. Clinical Characteristics of the Enrolled Patients

The patients' characteristics are summarized in Table 1. Among 546 patients, 250 patients (45.8%) were categorized as having IA. There were no statistical differences in gender distribution, HTN, DM, hyperlipidemia, and smoking between the two groups. Control subjects were younger than IA patients ( $p < 0.001$ ). For IA patients, the incidence of SAH and UIA was 151 (60.4%) and 99 (39.6%), respectively. Anterior circulation aneurysms accounted for the majority of the IAs ( $n = 221$ , 88.4%), consisting of the middle cerebral artery ( $n = 71$ ), the anterior communicating artery or the anterior cerebral artery ( $n = 59$ ), the internal carotid artery ( $n = 38$ ), or the posterior communicating artery ( $n = 53$ ).

**Table 1.** Baseline Characteristics for Study Population.

Variables <sup>a</sup>	Case (n = 250)	Control (n = 296)	P <sup>b</sup>
Female, N (%)	146 (58.4)	154 (52.0)	0.74
Age, years	59.3 ± 0.8	52.1 ± 1.0	<0.001
Hypertension, N (%)	93 (37.2)	88 (29.7)	0.865
Diabetes mellitus, N (%)	17 (6.8)	37 (12.5)	0.001
Hyperlipidemia, N (%)	29 (11.6)	27 (9.1)	0.476
Cigarette smoking, N (%)	26 (10.4)	37 (12.5)	0.615
Principal components, mean <sup>c</sup>			
Principal component 1	0.0014	−0.0012	0.169
Principal component 2	−0.0002	0.0001	0.656
Principal component 3	−0.0010	0.0008	0.039
Principal component 4	−0.0011	0.0009	0.031
Rupture status, N (%)			
UIA	99 (39.6)	-	-
SAH	151 (60.4)	-	-

SAH, subarachnoid hemorrhage; UIA, unruptured intracranial aneurysm. <sup>a</sup> Data are shown as the number of subjects (percentage) for discrete and categorical variables and mean ± standard error. <sup>b</sup> P values were estimated in the multivariate logistic regression model. <sup>c</sup> Principal components were estimated by performing the principal component analysis with four clusters.

### 3.2. GWAS and Single-cell eQTL Analysis

A total of 315 SNPs, including small indels, showed suggestive associations with p-values less than  $1 \times 10^{-5}$  in our GWAS after adjusting for confounder factors and four principal components in the enrolled patients (Figure 1 and Supplementary Table S1).

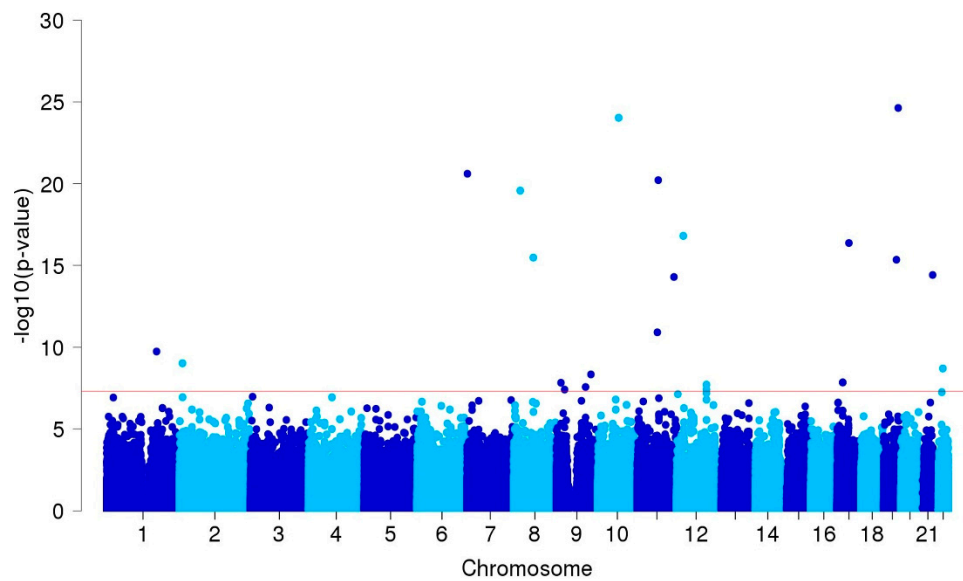


**Figure 1.** Manhattan plot of a genome-wide association study in 250 patients with intracranial aneurysms and 294 controls after adjusting for age, sex, hypertension, diabetes, hyperlipidemia, cigarette smoking, and four principal components. The red sub-line indicates the genome-wide significance threshold ( $P = 5 \times 10^{-8}$ ).

After removing pairwise linkage disequilibriums of less than 0.8, 29 out of those SNPs achieved a genome-wide significance threshold  $p$ -value of less than  $5 \times 10^{-8}$  (Table 2).

**Table 2.** Genome-wide associations of 29 SNPs with intracranial aneurysm.

Gene	Chr.	SNP	Class	M/m <sup>a</sup>	MAF <sup>b</sup>	OR <sup>c</sup>	L95 <sup>c</sup>	U95 <sup>c</sup>	P <sup>c</sup>	Power <sup>d</sup>
PRDM2	1p36.21	rs61775135	intron	C/A	0.16/0.41	0.32	0.23	0.43	3.6E-13	0.42
GBA	1q22	rs75822236	R535H	C/T	0.33/0.01	161.40	53.86	483.60	1.1E-19	1.00
FMO4	1q24.3	rs3737926	F281F	C/T	0.16/0.37	0.36	0.27	0.50	1.8E-10	0.32
RNF144A	2p25.1	rs6741819	intron	C/T	0.13/0.37	0.25	0.18	0.36	4.0E-14	0.72
FLJ45964	2q37.3	rs59626274	stop-gained	C/T	0.13/0.36	0.26	0.18	0.37	5.8E-14	0.71
LINC01237	2q37.3	rs78458145	intron	G/A	0.17/0.4	0.24	0.17	0.35	3.1E-15	0.68
SPCS3	4q34.2	rs17688188	intergenic	G/A	0.11/0.33	0.27	0.19	0.38	6.0E-13	0.73
TCF24	8q13.1	rs112859779	G141S	C/T	0.1/0.33	0.19	0.12	0.28	3.3E-16	0.94
C9orf92	9p22.3	rs12350582	intergenic	A/G	0.33/0.18	2.43	1.79	3.31	1.5E-08	0.20
LINGO2	9p21.1	rs56942085	intron	G/A	0.1/0.03	6.11	3.20	11.64	3.9E-08	0.78
TMOD1	9q22.33	rs1052270	intron	C/T	0.27/0.42	0.41	0.30	0.56	2.7E-08	0.15
SUSD1	9q31.3	rs79461840	intron	T/C	0.13/0.02	6.92	3.55	13.49	1.4E-08	0.65
LINC00474	9q33.1	rs4979583	intergenic	C/T	0.41/0.24	2.45	1.82	3.31	4.6E-09	0.24
OLFML2A	9q33.3	rs79134766	A208T	G/A	0.07/0.37	0.14	0.09	0.21	1.7E-19	0.96
MYEOV	11q13.3	rs76855873	intron	C/T	0.16/0.37	0.33	0.24	0.46	1.2E-11	0.43
ARHGAP32	11q24.3	rs371331393	stop-gained	G/A	0.32/0.02	43.57	21.84	86.95	9.3E-27	1.00
CD163L1	12p13.31	rs138525217	splice-site	C/T	0.31/0.01	75.98	32.13	179.70	6.2E-23	1.00
SLC2A14	12p13.31	rs118107419	intron	C/A	0.14/0.39	0.25	0.17	0.35	1.4E-14	0.67
DRAM1	12q23.2	rs7964241 <sup>e</sup>	intergenic	A/G	0.35/0.21	2.49	1.81	3.42	2.0E-08	0.25
CUL4A	13q34	rs74115822	intergenic	G/A	0.19/0.03	6.25	3.58	10.90	1.1E-10	0.80
LINC02130	16p13.12	rs11646803	intron	C/T	0.28/0.48	0.45	0.35	0.58	4.8E-10	0.06
LOC102724084	16q23.2	rs75861150	intron	T/C	0.02/0.16	0.14	0.07	0.28	1.3E-08	1.00
SCARF1	17p13.3	rs3744644	E639D	G/C	0.18/0.35	0.39	0.28	0.54	6.0E-09	0.26
MINK1	17p13.2	rs72835045	intron	G/A	0.11/0.33	0.25	0.17	0.37	1.7E-12	0.79
SLC47A1	17p11.2	rs2440154 <sup>e</sup>	intron	G/A	0.28/0.13	2.67	1.90	3.75	1.4E-08	0.26
NAPA-AS1	19q13.32	rs55800589	intron	G/C	0.32/0.4	0.38	0.29	0.49	3.4E-13	0.23
DSCAM	21q22.2	rs727333	intron	C/A	0.14/0.38	0.26	0.18	0.36	3.7E-14	0.69
LRRC3	21q22.3	rs116969723	P63P	G/A	0.11/0.35	0.24	0.16	0.34	3.8E-15	0.81
SLC5A4-AS1	22q12.3	rs117398778	intron	T/C	0.21/0.07	3.74	2.43	5.75	2.0E-09	0.56

Chr. chromosome; L95, lower 95% confidence interval; OR, odds ratio; U95, upper 95% confidence interval. <sup>a</sup> M/m, major/minor allele type; <sup>b</sup> MAF, minor allele frequency in case (left) and control (right); <sup>c</sup> OR, 95% confidence interval, and  $p$ -value were estimated in the multivariate logistic regression model after adjustment for age, sex, hypertension, diabetes, hyperlipidemia, cigarette smoking, and four principal components; <sup>d</sup> The statistical power for each SNP was estimated by performing the web-based Genetic Power Calculator (<http://zzz.bwh.harvard.edu/gpc/cc2.html>) using parameters, such as 5% prevalence of intracranial aneurysm, MAF in control, OR under an additive model, D-prime 0.8, 1:1.18 case-control ratio (296 controls/250 cases = 1.18), and type 1 error rate of  $5 \times 10^{-8}$  (genome-wide significance threshold); <sup>e</sup> One SNP shown in a pairwise linkage disequilibrium (LD,  $r^2 < 0.8$ ): rs7964241 and rs56168082 ( $r^2 = 0.81$ ); rs2440154 and rs2289668 ( $r^2 = 1.0$ ).

The nonsense variant having a stop-gain function, rs371331393 located on *ARHGAP32* (11q24.3), showed the most significant association for IA formation (OR = 43.57, 95% confidence interval (CI) 21.84–86.95;  $p = 9.3 \times 10^{-27}$ ) (Figure 2).

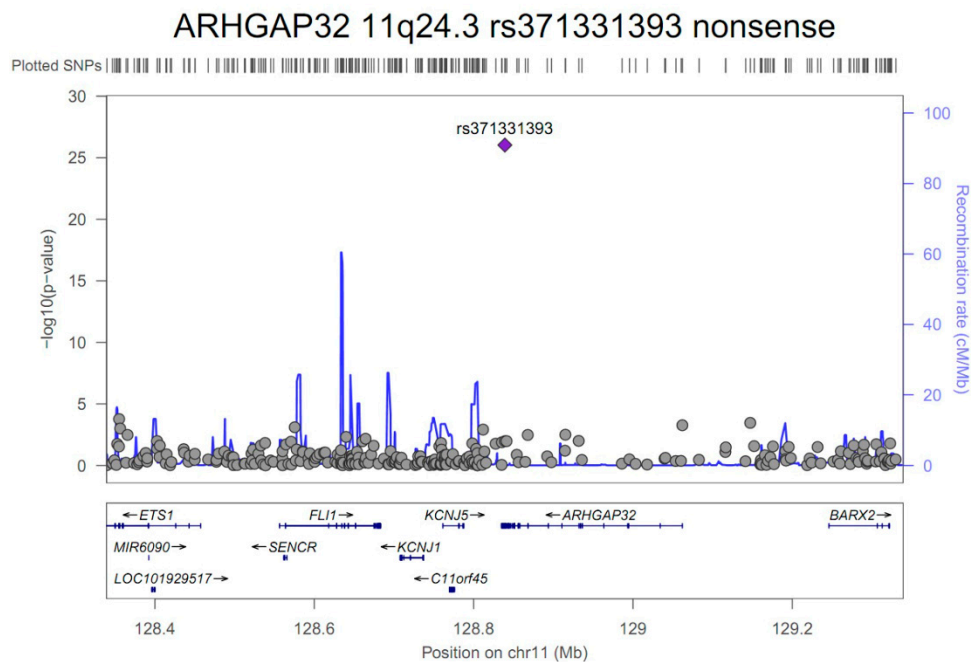


**Figure 2.** A regional plot of the rs371331393 (stop-gained mutation, *ARHGAP32*, 11q24.3) variant's position  $\pm$  500 kb shows associations with intracranial aneurysms in 250 patients and 294 controls after adjusting for age, sex, hypertension, diabetes, hyperlipidemia, cigarette smoking, and four principal components. The x- and y-axes indicate the chromosomal position (mega base, Mb) and  $-\log_{10}$  transformed *P*-values, respectively. The purple diamond indicates the rs371331393 variant demonstrating the most significant association in our genome-wide association study ( $P = 9.3 \times 10^{-27}$ ). The gray circles indicate other SNPs within 500 kb of the rs371331393 variant's position.

In addition, four SNPs—rs75822236 (R535H, *GBA*, 1q22), rs112859779 (G141S, *TCF24*, 8q13.1), rs79134766 (A208T, *OLFML2A*, 9q33.3), rs3744644 (E639D, *SCARF1*, 17p13.3), and an additional nonsense SNP rs59626274 (stop-gained, *FLJ45964*, 2q37.3)—demonstrated potential direct relationships with coding proteins in sequences. The rs75822236 SNP showed the strongest associations with the risk of IA formation (OR = 161.46, 95% CI 53.86–483.60;  $p = 1.1 \times 10^{-19}$ ). The “T” allele of this variant was rare in the control group compared with the “C” allele in patients with IA (MAF = 0.01 versus 0.33). The “T” allele in one splice acceptor and in transcript variant rs138525217 SNP located on the 3-prime untranslated region (UTR) of the *CD163L1* gene showed a rare occurrence and large effect size (MAF case/control = 0.31/0.01, OR = 75.98;  $p = 6.2 \times 10^{-23}$ ). Eight out of 29 SNPs reached sufficient statistical power greater than or equal to 0.8, while other SNPs were underpowered in this GWAS because of the small sample size (Table 2). Two out of 17 previously reported SNPs—the rs700651 intron variant of the *BOLL* gene (2q33.1) and the rs6841581 located near the 5-prime UTR of *EDNRA* (4q31.22)—were validated in our study ( $p = 0.008$  and  $6.5 \times 10^{-4}$ , respectively) (Supplementary Table S2). Although none of the SNPs reached a genome-wide significance threshold for IA rupture, one intron variant, the rs6990241 of the *SGCZ* gene (8p22), showed a suggestive association with aneurysm rupture (OR = 0.34, 95% CI 0.22–0.55;  $p = 8.5 \times 10^{-6}$ ) (Supplementary Figure S1).

In a subsequent single-cell eQTL analysis on at least 70 samples from 45 human tissues, three SNPs showed significant differences in expressions ( $p < 1 \times 10^{-5}$ ): rs6741819 (*RNF144A*, 2p25.1;  $p = 4.0 \times 10^{-14}$ ) (Figure 3A) was down-regulated in the adrenal gland tissue (175 samples, effect size =  $-0.36$ ,  $p = 1.5 \times 10^{-6}$ ) (Figure 3B), rs1052270 (*TMOD1*, 9q22.33;  $p = 2.7 \times 10^{-8}$ ) (Figure 3C) was up-regulated in the testis tissue (225 samples, effect size = 0.42,  $p = 8.6 \times 10^{-10}$ ) (Figure 3D), and rs6841581 (*EDNRA*, 4q31.22;  $p = 6.5 \times 10^{-4}$ ) (Supplementary Table S2 and Supplementary Figure S2A) was up-regulated in both the esophagus (*mucosa*) (358 samples, effect size = 0.38,  $p = 5.2 \times 10^{-12}$ ) (Supplementary

Figure S2B) and the skin in areas not exposed to the sun (*suprapubic*) (335 samples, effect size = 0.21,  $p = 1.2 \times 10^{-6}$ ) (Supplementary Figure S2C).

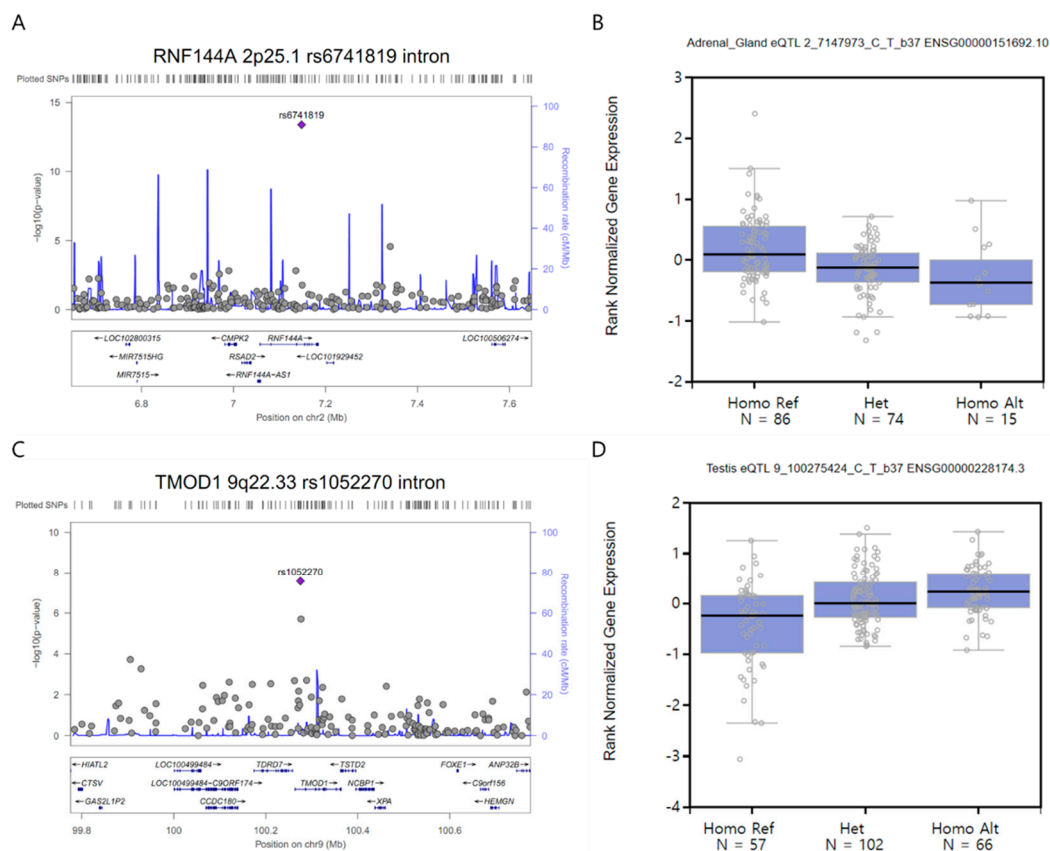


**Figure 3.** (A and C) A regional plot of (A) the rs6741819 (intron, *RNF144A*, 2p25.1) and (C) rs1052270 (intron, *TMOD1*, 9q22.33) variants ( $\pm 500$  kb) demonstrates associations with intracranial aneurysms in 250 patients and 294 controls after adjusting for age, sex, hypertension, diabetes, hyperlipidemia, cigarette smoking, and four principal components. The x- and y-axes indicate the chromosomal position (mega base, Mb) and  $-\log_{10}$  transformed  $P$ -values, respectively. The purple diamonds indicate the rs6741819 and rs1052270 variants with genome-wide associations in our study ( $p = 4.0 \times 10^{-14}$  and  $2.7 \times 10^{-8}$ , respectively). The gray circles indicate other SNPs within 500kb of the rs6990241 and rs1052270 variants' position. (B and D) The expression level of (B) rs6741819 and (D) rs1052270 variants in the adrenal gland ( $n = 175$ ) and testis ( $n = 225$ ) tissues, respectively, according to single-cell expression quantitative trait loci (eQTL) in the GTEx portal (<https://gtexportal.org/home>). The x- and y-axes indicate three genotypes for each variant and the rank-normalized gene expression level, respectively. The Reference (Ref) and Alternative (Alt) alleles of each variant's genotypes are equal to their major/minor alleles, respectively. Homo, homozygote; Het, heterozygote.

### 3.3. Gene Function and Network Analysis

In an analysis of gene function, 13 of 235 biological functions showed statistically significant GO terms ( $p < 0.05$ ) (Table 3).

**Table 3.** Gene enrichment functional analysis using candidate genes for susceptibility to intracranial aneurysms ( $p < 0.05$ ).

Biological Function <sup>a</sup>	P <sup>b</sup>	FDR, % <sup>b</sup>	Gene, N	Gene Set
<i>Biological process in ontology</i>				
GO: 0030154~cell differentiation	0.0117	16.8	10	EDNRA, LINGO2, CUL4A, SLC2A14, MINK1, SCARF1, BOLL, DSCAM, TMOD1, GBA
GO: 0031175~neuron projection development	0.0120	17.2	5	LINGO2, MINK1, SCARF1, DSCAM, GBA
GO: 0048468~cell development	0.0181	24.8	7	EDNRA, LINGO2, MINK1, SCARF1, DSCAM, TMOD1, GBA
GO: 0016358~dendrite development	0.0192	26.1	3	MINK1, SCARF1, DSCAM
GO: 0048869~cellular developmental process	0.0209	28.1	10	EDNRA, LINGO2, CUL4A, SLC2A14, MINK1, SCARF1, BOLL, DSCAM, TMOD1, GBA
GO: 0048666~neuron development	0.0210	28.3	5	LINGO2, MINK1, SCARF1, DSCAM, GBA
GO: 0007275~multicellular organism development	0.0260	33.8	11	EDNRA, LINGO2, CUL4A, SLC2A14, MINK1, PRDM2, SCARF1, BOLL, DSCAM, TMOD1, GBA
GO: 0051130~positive regulation of cellular component organization	0.0406	47.7	5	LINGO2, CUL4A, SCARF1, DSCAM, GBA
GO: 0030182~neuron differentiation	0.0454	51.6	5	LINGO2, MINK1, SCARF1, DSCAM, GBA
<i>Cellular component in ontology</i>				
GO:0044425~membrane part	0.0088	9.7	15	FMO4, RNF144A, LINGO2, EDNRA, LRRC3, ARHGAP32, CD163L1, SLC2A14, SUSD1, SPCS3, MINK1, SLC47A1, DRAM1, SCARF1, DSCAM
GO:0016021~integral component of membrane	0.0160	16.9	13	FMO4, RNF144A, LINGO2, EDNRA, LRRC3, CD163L1, SLC2A14, SUSD1, SPCS3, SLC47A1, DRAM1, SCARF1, DSCAM
GO:0031224~intrinsic component of membrane	0.0186	19.4	13	FMO4, RNF144A, LINGO2, EDNRA, LRRC3, CD163L1, SLC2A14, SUSD1, SPCS3, SLC47A1, DRAM1, SCARF1, DSCAM
GO:0016020~membrane	0.0205	21.1	17	RNF144A, LRRC3, SUSD1, SLC2A14, MINK1, SLC47A1, SCARF1, FMO4, EDNRA, LINGO2, ARHGAP32, CD163L1, SPCS3, DRAM1, DSCAM, TMOD1, GBA

FDR, false discovery rate; GO, gene ontology. <sup>a</sup> Functional categories in gene ontology; <sup>b</sup> Fisher's exact  $p$ -value and FDR of each biological function were estimated by DAVID v.6.8 program.

Seven out of 31 IA-predicting genes—*FLJ45964*, *LINC01237*, *LINC00474*, *LINC02130*, *LOC102724084*, *NAPA-AS1*, and *SLC5A4-AS1*—were not available in either DAVID or STRING databases. Among those terms, the GO: 0044425 containing a “membrane part” function in the cellular component ontology was highly enriched in the cluster involving 15 genes ( $p = 0.0088$ , FDR = 9.7%). In particular, five genes, *EDNRA*, *LINGO2*, *GBA*, *DSCAM*, and *SCARF1*, played various roles in the development of cells, neurons, and cell membranes. A network analysis further supported the evidence of IA-predicting genes, including the three crucial genes *EDNRA*, *LINGO2*, and *GBA* (Supplementary Figure S3).

#### 4. Discussion

In this study, we investigated 29 novel genes and found 8 genetic variants demonstrating sufficient statistical power (above 80%)—*GBA*, *TCF24*, *OLFML2A*, *ARHGAP32*, *CD163L1*, *CUL4A*, *LOC102724084*, and *LRRC3*—and 5 variants with marginal statistical power (70% to 80%)—*RNF144A*, *FLJ45964*, *SPCS3*, *LINGO2*, and *MINK1*—for IA susceptibility. The *ARHGAP32* gene (also called p250GAP), containing the most significant nonsense mutation (rs371331393), regulates Rho GTPase activating protein and NMDA receptor signaling involved in RhoGAP. Rho GTPases are associated with HTN through the regulation of vascular tone [24]. Bai et al. [25] showed Rho-specific GAP expression in smooth muscle cells in human and mice. *ARHGAP42* knockout mice experienced significantly elevated blood pressure and cardiac contractility. In addition, the blood pressure increased significantly in response to endothelin-1 and angiotensin II [24,25]. Without a doubt, HTN is a risk factor for aneurysm formation and growth. Chronic HTN can cause intimal thickening with degeneration of the internal elastic lamina, causing a focal weakness of the arterial wall [26]. Thus, genes regulating Rho GTPase activity are likely involved in the pathogenesis of IA. Although the loci 11q.24.3 was statistically significant after adjusting for covariates including HTN, further study about the role of *ARHGAP32* gene in IA pathogenesis is required.

Glucocerebrosidase (*GBA*) mutation is a well-known risk factor for PD. Malek et al. [27] reported that patients with pathogenic *GBA* mutations, including L444P, showed a 5 year earlier onset of PD than non-carriers. In addition, mild and severe heterozygous *GBA* mutations also affect the risk of PD and age of onset [28]. Lysosomal dysfunction, particularly lysosomal storage disorder due to lysosomal gene deficiency, is often a pathognomonic sign of neurodegenerative disease [29]. However, in ischemic or hemorrhagic strokes, the relationship to lysosomal dysfunction has not been well investigated, and prior studies have mainly focused on autophagic and lysosomal pathways after cerebral ischemia. Gu et al. [30] reported that autophagic bodies and lysosomes accumulated in neurons within 4 hours after an ischemic injury and gradually dissipated over time. Western blotting revealed increased levels of light chain 3-II and cathepsin B 4 hours after ischemic injury. Considering that matrix-degrading enzymes of lysosomal cysteine cathepsins are related to tissue remodeling and tumor invasion [31], further research on the impact of lysosomal mutation on IA pathogenesis is necessary. Also, the *MINK1* gene contributes to the mediation of mitogen-activated protein kinase signaling, as well as platelet activation and thrombus formation [32]. Intraluminal thrombi are known to contribute to aneurysm growth and rupture in abdominal aortic aneurysms (AAA), and thus, may play a role in IA as well [33]. Hansen et al. [33] measured platelet activation potential using computational fluid dynamics, but failed to demonstrate significant differences in stress-induced action potentials within aneurysm walls under resting or exercising conditions. Since platelet aggregation is more evident in smaller arteries [34] and IAs have a different mechanical flow pattern compared with abdominal aortic aneurysms, further study on the relationship between platelet activation and aneurysm formation is required. In addition, other novel gene variants should be investigated to identify their mechanism and clinical relevance to IA formation.

Abnormal extracellular matrix (ECM) remodeling and subsequent ECM degradation as well as endothelial injury in response to hemodynamic stress and growth factors, including transforming growth factor- $\beta$  (*TGF  $\beta$* ), are related to IA formation and growth [35]. Connective tissue growth

factor (*CTGF*, also known as *CCN2*) regulates vascular structural remodeling, cell proliferation, and differentiation.  $TGF\ \beta$  is a well-known regulator of *CTGF* expression. Ungvari et al. [35] suggested that ECM remodeling caused by high *CTGF* expression in the vascular wall is responsible for age-related large arterial pathogenesis such as atherogenesis and aneurysm formation. Although definite mutations in the *TGF*  $\beta$  receptors genes (*TGFBR1* and *TGFBR2*) were not noted in familial IA patients, some novel variants, including *TGFBR3*/Betaglycan, were noted [36]. Olfactomedin, like 2A (*OLFML2A*), one of the olfactomedin domain-containing proteins, play a role in cellular differentiation and is mediated by ECM components [37]. *OLFML2A* has a tissue-specific expression, without expression in neuronal tissue. The function of *OLFML2* protein has not been well characterized. Among ECM components, *OLFML2* proteins bind to chondroitin sulphate-E and heparin preferentially [38,39]. Therefore, additional studies about the potential role of *CTGF* and *OLFML2A* in the process of ECM remodeling in IA development may be elucidating.

Endothelial injury is known to precede IA formation [40]. In such environments, clearance of apoptotic cells is important for tissue homeostasis, preventing morphological changes from a fusiform to a column shape [41,42]. Scavenger receptor class F, member 1 (*SCARF1*) binds to various endogenous (e.g., modified low-density lipoproteins, apoptotic cells, and heat shock proteins) and exogenous ligands of bacterial and viral antigens. *SCARF1* plays a crucial role in atherosclerosis, endothelial injury/dysfunction, inflammation, and host innate immunity, predominantly binding to carbamylated LDLs with its proatherogenic effect on human endothelial cells [42]. In our GWAS, mutations in *SCARF1* polymorphism, containing of common coding variant (rs3744644, E639D), showed a high correlation with IA formation, but this finding was underpowered. Therefore, the associations between *SCARF1* polymorphism and IA formation need to be studied in a larger population.

There exist genetic differences between inter-populations of the same ethnicity (i.e., Asians), and/or intra-population (i.e., Chinese populations) [43], as well as between different ethnicities, such as Asian and Caucasian populations [14]. In prior studies, Koreans showed different candidate SNPs for IA formation compared with the Japanese and Chinese population, as well as with the European population. Hong et al. [18] investigated four candidate SNPs located near or on the *SOX17* gene. Among them, only one SNP, the minor C allele of rs1072737 had significant association for IA in Koreans. With the elastin (*ELN*) gene, rs2071307 (Gly422Ser) was not associated with Korean IA, although a minor A allele of rs2071307 was significantly associated with Chinese IA [44]. We further evaluated previously reported SNPs in our results. Among the possible susceptible loci including 4q31.23, 9p21.3, and 8q11, which were mentioned in the previous reports [13], only two loci, rs700651 in the intron of *BOLL* [9] and rs6841581 near the 5-prime UTR of *EDNRA* [12], were replicated in our GWAS (Supplemental Table S2). Specifically, expression of the common susceptible "C" allele of the rs6841581 in the *EDNRA* gene, which is likely to inhibit transcription of *EDNRA* [12], was down-regulated in esophagus and skin tissues, and correlated with an increased risk for IA formation in our study. Interactions of endothelin-1 (EDN-1) and *EDNRA* were reported to function in IA pathogenesis and cerebrovascular vasospasms after SAH [45]. Elevated plasma levels of EDN-1 highly correlated with SAH patients developing sustainable vasospasms in the cerebrovascular inflammatory system [46]. In a subsequent GWAS, although none of our findings showed a genome-wide significance with SAH in patients with IA, we discovered that there was a suggestive association with the *SGCZ* gene, which is a component of the vascular smooth muscle sarcoglycan complex that contributes to muscular dystrophy pathogenesis [47] and should be further investigated for its contribution to SAH formation at the molecular level.

In our study, transcription factor 24 (*TCF24*) was significantly related to IA formation, indicating protective effects. Associations between *TCF24* and IA formation have not been investigated before. *TCF24*, rs182838111 located at chromosome 8, increased the risk of Alzheimer's disease via family meta-analyses [48]. In our analysis, patients diagnosed with Alzheimer's disease were not enrolled as control subjects, although the potential inclusion of late-onset Alzheimer patients cannot be discounted. Accordingly, interpretation of GWAS, in particular involving *TCF24*, warrants caution. Different

baseline characteristics, particularly patients' age and DM, may affect aneurysm incidence. In our study, patients harboring IA were older with had a lower incidence of DM compared with control subjects. Age at diagnosis could be translated into the duration of follow-up period. A higher incidence of aneurysm, irrespective of aneurysm rupture, was noted in those over 75 [49]. Moreover, the patients' age and aneurysm size were well correlated with  $F^{14}C$  levels in SAH patients, indicating high turnover in collagen in the aneurysm walls [50]. Accordingly, additional studies regarding age stratification and IA formation would be necessary to further evaluate these relationships. Regarding DM in our study, it seemed to have a protective effect for IA formation (6.8% in IA vs. 12.5% in controls;  $p = 0.001$ ). Dattani et al. [51] reported a negative association between AAA and DM. In addition, medications to treat DM can inhibit AAA formation and growth [51]. Therefore, further studies regarding DM and medications on IA formation and growth are needed.

There are some limitations to this study. Our GWAS enrolled 250 patients with IA and 294 controls from Korean adults selected from hospitalization and community-based cohorts. Our findings may have been underpowered to identify genetic variations for susceptibility to IA or SAH with the small sample size [52], even though some of the variants reached the genome-wide significance threshold with large effect sizes. Thus, further studies are warranted in a larger population-based cohort of patients and should be replicated in an independent cohort. In addition, our significant findings should be validated functionally at the molecular or cellular level to identify their roles in the multifactorial mechanical pathogenesis of IA formation. Finally, we did not thoroughly examine the patients who develop IA at a young age. Given the critical relevance of early age-of-onset for IA, future studies in patients younger than 30 years will help elucidate important clues to the genetic architecture for IA occurring in the younger population. Despite these limitations, our findings may ultimately lead to the development of targeted therapeutic and preventive diagnosis for cerebrovascular diseases.

## 5. Conclusions

This GWAS is a powerful application of the Asian-specific PMRA chip that contains large-scale variations, including clinical and disease-associated markers. The evidence of novel candidate genes with Korean-specific variations suggest a genetic component to susceptibility to IA in Korean adults. Some of these variations, including *GBA*, *ARHGAP32*, *OLFML2A*, *SCARF1*, and *MINK1*, have been implicated to indirectly or directly contribute to IA pathogenesis through the inflammatory or cerebrovascular system in human blood vessels. Further study is necessary to validate these results in independent populations. Ultimately, a comprehensive approach integrating clinically relevant elements and genetic components may provide beneficial clues to evaluate the risk assessment and preventive medicine for the development of IA and subsequent rupture.

**Supplementary Materials:** The following are available online at <http://www.mdpi.com/2077-0383/8/2/275/s1>. Table S1. 315 SNP Association (Excel file); Table S2. Associations of 17 previously reported SNPs with intracranial aneurysms in our genome-wide association study; Figure S1: A regional plot of the rs6990241 (intron, *SGCZ*, 8p22) variant's position  $\pm 500$  kb demonstrates associations with subarachnoid hemorrhage in 250 patients with intracranial aneurysm after adjusting for age, sex, hypertension, diabetes, hyperlipidemia, cigarette smoking, and four principal components; Figure S2: A regional plot of (A) the reported SNP, rs6841581 (near UTR-5, *EDNRA*, 4q31.22) variant's position  $\pm 500$  kb demonstrating a replicated association with intracranial aneurysms in 250 patients and 294 controls after adjusting for age, sex, hypertension, diabetes, hyperlipidemia, cigarette smoking, and four principal components; Figure S3: Shown here is a network of multiple protein-coding gene-gene interactions using 25 out of 31 candidate genes for susceptibility to intracranial aneurysms (six genes, *LINC01237*, *LINC00474*, *LINC02130*, *LOC102724084*, *NAPA-AS1*, and *SLC5A4-AS1*, were not available in the STRING v.10.5 database; ENSG00000196758 indicates the *FLJ45964* gene) (*Homo sapiens*).

**Author Contributions:** Conceptualization, J.P.J.; Methodology, K.B.J., and C.B.S.; Validation, Y.J.S., and C.H.J.; Formal analysis H.E.P.; Writing-Original draft preparation, H.E.P and K.S.H.; Project administration; Supervision. J.P.J.

**Funding:** This research was supported by a BioGreen21 (PJ01313901) grant from the Rural Development Administration and National Research Foundation of Korea and funded by the Ministry of Science, Information and Communication Technologies and Future Planning of the Government of Korea (No. 2017M3A9E8033223).

**Acknowledgments:** The Genotype-Tissue Expression (GTEx) Project was supported by the Common Fund of the Office of the Director of the National Institutes of Health, and by NCI, NHGRI, NHLBI, NIDA, NIMH, and NINDS. The data used for the eQTL analyses described in this manuscript were obtained from the GTEx Portal on 01/15/2019.

**Conflicts of Interest:** The authors declare no conflict of interest.

## References

1. Vlak, M.H.; Algra, A.; Brandenburg, R.; Rinkel, G.J. Prevalence of unruptured intracranial aneurysms, with emphasis on sex, age, comorbidity, country, and time period: A systematic review and meta-analysis. *Lancet Neurol.* **2011**, *10*, 626–636. [[CrossRef](#)]
2. Katati, M.J.; Santiago-Ramajo, S.; Perez-Garcia, M.; Meersmans-Sanchez Jofre, M.; Vilar-Lopez, R.; Coin-Mejias, M.A.; Caracuel-Romero, A.; Arjona-Moron, V. Description of quality of life and its predictors in patients with aneurysmal subarachnoid hemorrhage. *Cerebrovasc Dis.* **2007**, *24*, 66–73. [[CrossRef](#)] [[PubMed](#)]
3. Nahed, B.V.; Bydon, M.; Ozturk, A.K.; Bilguvar, K.; Bayrakli, F.; Gunel, M. Genetics of intracranial aneurysms. *Neurosurgery* **2007**, *60*, 213–225. [[CrossRef](#)] [[PubMed](#)]
4. Caranci, F.; Briganti, F.; Cirillo, L.; Leonardi, M.; Muto, M. Epidemiology and genetics of intracranial aneurysms. *Eur. J. Radiol.* **2013**, *82*, 1598–1605. [[CrossRef](#)] [[PubMed](#)]
5. Onda, H.; Kasuya, H.; Yoneyama, T.; Takakura, K.; Hori, T.; Takeda, J.; Nakajima, T.; Inoue, I. Genomewide-linkage and haplotype-association studies map intracranial aneurysm to chromosome 7q11. *Am. J. Hum. Genet.* **2001**, *69*, 804–819. [[CrossRef](#)] [[PubMed](#)]
6. Olson, J.M.; Vongpunsawad, S.; Kuivaniemi, H.; Ronkainen, A.; Hernesniemi, J.; Ryyanen, M.; Kim, L.L.; Tromp, G. Search for intracranial aneurysm susceptibility gene(s) using Finnish families. *BMC Med. Genet.* **2002**, *3*, 7. [[CrossRef](#)]
7. Nahed, B.V.; Seker, A.; Guclu, B.; Ozturk, A.K.; Finberg, K.; Hawkins, A.A.; DiLuna, M.L.; State, M.; Lifton, R.P.; Gunel, M. Mapping a Mendelian form of intracranial aneurysm to 1p34.3-p36.13. *Am. J. Hum. Genet.* **2005**, *76*, 172–179. [[CrossRef](#)] [[PubMed](#)]
8. Yamada, S.; Utsunomiya, M.; Inoue, K.; Nozaki, K.; Inoue, S.; Takenaka, K.; Hashimoto, N.; Koizumi, A. Genome-wide scan for Japanese familial intracranial aneurysms: linkage to several chromosomal regions. *Circulation* **2004**, *110*, 3727–3733. [[CrossRef](#)] [[PubMed](#)]
9. Bilguvar, K.; Yasuno, K.; Niemela, M.; Ruigrok, Y.M.; von Und, Z.; Fraunberg, M.; van Duijn, C.M.; Tajima, A.; Laakso, A.; Hata, A.; et al. Susceptibility loci for intracranial aneurysm in European and Japanese populations. *Nat. Genet.* **2008**, *40*, 1472–1477. [[CrossRef](#)] [[PubMed](#)]
10. Akiyama, K.; Narita, A.; Nakaoka, H.; Cui, T.; Takahashi, T.; Yasuno, K.; Tajima, A.; Kirschke, B.; Yamamoto, K.; Kasuya, H.; et al. Genome-wide association study to identify genetic variants present in Japanese patients harboring intracranial aneurysms. *J. Hum. Genet.* **2010**, *55*, 656–661. [[CrossRef](#)] [[PubMed](#)]
11. Yasuno, K.; Bilguvar, K.; Bijlenga, P.; Low, S.K.; Kirschke, B.; Auburger, G.; Simon, M.; Krex, D.; Arlier, Z.; Nayak, N.; et al. Genome-wide association study of intracranial aneurysm identifies three new risk loci. *Nat. Genet.* **2010**, *42*, 420–425. [[CrossRef](#)] [[PubMed](#)]
12. Low, S.K.; Takahashi, A.; Cha, P.C.; Zembutsu, H.; Kamatani, N.; Kubo, M.; Nakamura, Y. Genome-wide association study for intracranial aneurysm in the Japanese population identifies three candidate susceptible loci and a functional genetic variant at EDNRA. *Hum. Mol. Genet.* **2012**, *21*, 2102–2110. [[CrossRef](#)] [[PubMed](#)]
13. Alg, V.S.; Sofat, R.; Houlden, H.; Werring, D.J. Genetic risk factors for intracranial aneurysms: A meta-analysis in more than 116,000 individuals. *Neurology* **2013**, *80*, 2154–2165. [[CrossRef](#)] [[PubMed](#)]
14. Huang, T.; Shu, Y.; Cai, Y.D. Genetic differences among ethnic groups. *BMC Genomics* **2015**, *16*, 1093. [[CrossRef](#)] [[PubMed](#)]
15. Lee, J.Y.; Kim, T.H.; Yang, P.S.; Lim, H.E.; Choi, E.K.; Shim, J.; Shin, E.; Uhm, J.S.; Kim, J.S.; Joung, B.; et al. Korean atrial fibrillation network genome-wide association study for early-onset atrial fibrillation identifies novel susceptibility loci. *Eur. Heart J.* **2017**, *38*, 2586–2594. [[CrossRef](#)] [[PubMed](#)]
16. Kim, C.H.; Jeon, J.P.; Kim, S.E.; Choi, H.J.; Cho, Y.J. Endovascular Treatment with Intravenous Thrombolysis versus Endovascular Treatment Alone for Acute Anterior Circulation Stroke: A Meta-Analysis of Observational Studies. *J. Korean Neurosurg. Soc.* **2018**, *61*, 467–473. [[CrossRef](#)] [[PubMed](#)]

17. Hong, E.P.; Jeon, J.P.; Kim, S.E.; Yang, J.S.; Choi, H.J.; Kang, S.H.; Cho, Y.J. A Novel Association between Lysyl Oxidase Gene Polymorphism and Intracranial Aneurysm in Koreans. *Yonsei Med. J.* **2017**, *58*, 1006–1011. [[CrossRef](#)] [[PubMed](#)]
18. Hong, E.P.; Kim, B.J.; Kim, C.; Choi, H.J.; Jeon, J.P. Association of SOX17 Gene Polymorphisms and Intracranial Aneurysm: A Case-Control Study and Meta-Analysis. *World Neurosurg.* **2018**, *110*, e823–e829. [[CrossRef](#)] [[PubMed](#)]
19. Chang, C.C.; Chow, C.C.; Tellier, L.C.; Vattikuti, S.; Purcell, S.M.; Lee, J.J. Second-generation PLINK: Rising to the challenge of larger and richer datasets. *Gigascience* **2015**, *4*, 7. [[CrossRef](#)] [[PubMed](#)]
20. GTEx Consortium. Human genomics. The Genotype-Tissue Expression (GTEx) pilot analysis: Multitissue gene regulation in humans. *Science* **2015**, *348*, 648–660. [[CrossRef](#)] [[PubMed](#)]
21. Pruim, R.J.; Welch, R.P.; Sanna, S.; Teslovich, T.M.; Chines, P.S.; Gliedt, T.P.; Boehnke, M.; Abecasis, G.R.; Willer, C.J. LocusZoom: Regional visualization of genome-wide association scan results. *Bioinformatics* **2010**, *26*, 2336–22337. [[CrossRef](#)] [[PubMed](#)]
22. Dennis, G., Jr.; Sherman, B.T.; Hosack, D.A.; Yang, J.; Gao, W.; Lane, H.C.; Lempicki, R.A. DAVID: Database for Annotation, Visualization, and Integrated Discovery. *Genome Biol.* **2003**, *4*, P3. [[CrossRef](#)] [[PubMed](#)]
23. Szklarczyk, D.; Franceschini, A.; Wyder, S.; Forslund, K.; Heller, D.; Huerta-Cepas, J.; Simonovic, M.; Roth, A.; Santos, A.; Tsafou, K.P.; et al. STRING v10: Protein-protein interaction networks, integrated over the tree of life. *Nucleic Acids Res.* **2015**, *4*, D447–D452. [[CrossRef](#)] [[PubMed](#)]
24. Loirand, G.; Pacaud, P. Involvement of Rho GTPases and their regulators in the pathogenesis of hypertension. *Small GTPases* **2014**, *5*, 1–10. [[CrossRef](#)] [[PubMed](#)]
25. Bai, X.; Lenhart, K.C.; Bird, K.E.; Suen, A.A.; Rojas, M.; Kakoki, M.; Li, F.; Smithies, O.; Mack, C.P.; Taylor, J.M. The smooth muscle-selective RhoGAP GRAF3 is a critical regulator of vascular tone and hypertension. *Nat. Commun.* **2013**, *4*, 2910. [[CrossRef](#)] [[PubMed](#)]
26. Inci, S.; Spetzler, R.F. Intracranial aneurysms and arterial hypertension: A review and hypothesis. *Surg. Neurol.* **2000**, *53*, 530–540. [[CrossRef](#)]
27. Malek, N.; Weil, R.S.; Bresner, C.; Lawton, M.A.; Grosset, K.A.; Tan, M.; Bajaj, N.; Barker, R.A.; Burn, D.J.; Foltynie, T.; et al. Features of GBA-associated Parkinson's disease at presentation in the UK Tracking Parkinson's study. *J. Neurol. Neurosurg. Psychiatry* **2018**, *89*, 702–709. [[CrossRef](#)] [[PubMed](#)]
28. Gan-Or, Z.; Amshalom, I.; Kilariski, L.L.; Bar-Shira, A.; Gana-Weisz, M.; Mirelman, A.; Arder, K.; Bressman, S.; Giladi, N.; Orr-Urtreger, A. Differential effects of severe vs mild GBA mutations on Parkinson disease. *Neurology* **2015**, *84*, 880–887. [[CrossRef](#)] [[PubMed](#)]
29. Bae, E.J.; Yang, N.Y.; Lee, C.; Lee, H.J.; Kim, S.; Sardi, S.P.; Lee, S.J. Loss of glucocerebrosidase 1 activity causes lysosomal dysfunction and alpha-synuclein aggregation. *Exp. Mol. Med.* **2015**, *47*, e153. [[CrossRef](#)] [[PubMed](#)]
30. Gu, Z.; Sun, Y.; Liu, K.; Wang, F.; Zhang, T.; Li, Q.; Shen, L.; Zhou, L.; Dong, L.; Shi, N.; et al. The role of autophagic and lysosomal pathways in ischemic brain injury. *Neural Regen. Res.* **2013**, *23*, 2117–2125.
31. Tu, C.; Ortega-Cava, C.F.; Chen, G.; Fernandes, N.D.; Cavallo-Medved, D.; Sloane, B.F.; Band, V.; Band, H. Lysosomal cathepsin B participates in the podosome-mediated extracellular matrix degradation and invasion via secreted lysosomes in v-Src fibroblasts. *Cancer Res.* **2008**, *68*, 9147–9156. [[CrossRef](#)] [[PubMed](#)]
32. Yue, M.; Luo, D.; Yu, S.; Liu, P.; Zhou, Q.; Hu, M.; Liu, Y.; Wang, S.; Huang, Q.; Niu, Y.; et al. Misshapen/NIK-related kinase (MINK1) is involved in platelet function, hemostasis, and thrombus formation. *Blood* **2016**, *127*, 927–937. [[CrossRef](#)] [[PubMed](#)]
33. Hansen, K.B.; Arzani, A.; Shadden, S.C. Mechanical platelet activation potential in abdominal aortic aneurysms. *J. Biomech. Eng.* **2015**, *137*, 041005. [[CrossRef](#)] [[PubMed](#)]
34. Biasetti, J.; Spazzini, P.G.; Hedin, U.; Gasser, T.C. Synergy between shear-induced migration and secondary flows on red blood cells transport in arteries: considerations on oxygen transport. *J. R. Soc. Interface.* **2014**, *11*, 20140403. [[CrossRef](#)] [[PubMed](#)]
35. Ungvari, Z.; Valcarcel-Ares, M.N.; Tarantini, S.; Yabluchanskiy, A.; Fulop, G.A.; Kiss, T.; Csiszar, A. Connective tissue growth factor (CTGF) in age-related vascular pathologies. *Geroscience* **2017**, *39*, 491–498. [[CrossRef](#)] [[PubMed](#)]
36. Santiago-Sim, T.; Mathew-Joseph, S.; Pannu, H.; Milewicz, D.M.; Seidman, C.E.; Seidman, J.G.; Kim, D.H. Sequencing of TGF-beta pathway genes in familial cases of intracranial aneurysm. *Stroke* **2009**, *40*, 1604–1611. [[CrossRef](#)] [[PubMed](#)]

37. Anholt, R.R. Olfactomedin proteins: Central players in development and disease. *Front. Cell Dev. Biol.* **2014**, *2*, 6. [[CrossRef](#)] [[PubMed](#)]
38. Furutani, Y.; Manabe, R.; Tsutsui, K.; Yamada, T.; Sugimoto, N.; Fukuda, S.; Kawai, J.; Sugiura, N.; Kimata, K.; Hayashizaki, Y.; et al. Identification and characterization of photomedins: Novel olfactomedin-domain-containing proteins with chondroitin sulphate-E-binding activity. *Biochem. J.* **2005**, *389*, 675–684. [[CrossRef](#)] [[PubMed](#)]
39. Tomarev, S.I.; Nakaya, N. Olfactomedin domain-containing proteins: Possible mechanisms of action and functions in normal development and pathology. *Mol. Neurobiol.* **2009**, *40*, 122–138. [[CrossRef](#)] [[PubMed](#)]
40. Li, M.H.; Li, P.G.; Huang, Q.L.; Ling, J. Endothelial injury preceding intracranial aneurysm formation in rabbits. *West Indian Med. J.* **2014**, *63*, 167–171. [[PubMed](#)]
41. Ramirez-Ortiz, Z.G.; Pendergraft, W.F., 3rd; Prasad, A.; Byrne, M.H.; Iram, T.; Blanchette, C.J.; Luster, A.D.; Hacohen, N.; El Khoury, J.; Means, T.K. The scavenger receptor SCARF1 mediates the clearance of apoptotic cells and prevents autoimmunity. *Nat. Immunol.* **2013**, *14*, 917–926. [[CrossRef](#)] [[PubMed](#)]
42. Patten, D.A. SCARF1: A multifaceted, yet largely understudied, scavenger receptor. *Inflamm. Res.* **2018**, *67*, 627–632. [[CrossRef](#)] [[PubMed](#)]
43. HUGO Pan-Asian SNP Consortium; Abdulla, M.A.; Ahmed, I.; Assawamakin, A.; Bhak, J.; Brahmachari, S.K.; Calacal, G.C.; Chaurasia, A.; Chen, C.H.; Chen, J.; et al. Indian Genome Variation Consortium. Mapping human genetic diversity in Asia. *Science* **2009**, *326*, 1541–1545. [[PubMed](#)]
44. Yang, S.; Wang, T.; You, C.; Liu, W.; Zhao, K.; Sun, H.; Mao, B.; Li, X.; Xiao, A.; Mao, X.; et al. Association of polymorphisms in the elastin gene with sporadic ruptured intracranial aneurysms and unruptured intracranial aneurysms in Chinese patients. *Int. J. Neurosci.* **2013**, *123*, 454–458. [[CrossRef](#)] [[PubMed](#)]
45. Yu, J.C.; Pickard, J.D.; Davenport, A.P. Endothelin ETA receptor expression in human cerebrovascular smooth muscle cells. *Br. J. Pharmacol.* **1995**, *116*, 2441–2446. [[CrossRef](#)] [[PubMed](#)]
46. Fassbender, K.; Hodapp, B.; Rossol, S.; Bertsch, T.; Schmeck, J.; Schutt, S.; Fritzing, M.; Horn, P.; Vajkoczy, P.; Wendel-Wellner, M.; et al. Endothelin-1 in subarachnoid hemorrhage: An acute-phase reactant produced by cerebrospinal fluid leukocytes. *Stroke* **2000**, *31*, 2971–2975. [[CrossRef](#)] [[PubMed](#)]
47. Wheeler, M.T.; Zarnegar, S.; McNally, E.M. Zeta-sarcoglycan, a novel component of the sarcoglycan complex, is reduced in muscular dystrophy. *Hum. Mol. Genet.* **2002**, *11*, 2147–2154. [[CrossRef](#)] [[PubMed](#)]
48. Herold, C.; Hooli, B.V.; Mullin, K.; Liu, T.; Roehr, J.T.; Mattheisen, M.; Parrado, A.R.; Bertram, L.; Lange, C.; Tanzi, R.E. Family-based association analyses of imputed genotypes reveal genome-wide significant association of Alzheimer’s disease with OSBPL6, PTPRG, and PDCL3. *Mol. Psychiatry* **2016**, *21*, 1608–1612. [[CrossRef](#)] [[PubMed](#)]
49. Asaithambi, G.; Adil, M.M.; Chaudhry, S.A.; Qureshi, A.I. Incidences of unruptured intracranial aneurysms and subarachnoid hemorrhage: Results of a statewide study. *J. Vasc. Interv. Neurol.* **2014**, *7*, 14–17. [[PubMed](#)]
50. Etminan, N.; Dreier, R.; Buchholz, B.A.; Bruckner, P.; Steiger, H.J.; Hanggi, D.; Macdonald, R.L. Exploring the age of intracranial aneurysms using carbon birth dating: Preliminary results. *Stroke* **2013**, *44*, 799–802. [[CrossRef](#)] [[PubMed](#)]
51. Dattani, N.; Sayers, R.D.; Bown, M.J. Diabetes mellitus and abdominal aortic aneurysms: A review of the mechanisms underlying the negative relationship. *Diab. Vasc. Dis. Res.* **2018**, *15*, 367–374. [[CrossRef](#)] [[PubMed](#)]
52. Hong, E.P.; Park, J.W. Sample size and statistical power calculation in genetic association studies. *Genomics Inform.* **2012**, *10*, 117–122. [[CrossRef](#)] [[PubMed](#)]

